

# P3A.1 RELATIONSHIPS BETWEEN THE MICROPHYSICS OF PRECIPITATING CLOUD SYSTEMS AND THEIR RADAR REFLECTIVITY PATTERNS

Tristan S. L'Ecuyer\*, Christian Kummerow, and Hirohiko Masunaga  
Colorado State University, Fort Collins, Colorado

## 1. INTRODUCTION

Variability in the global distribution of precipitation is recognized as a key element in assessing the impact climate change on the environment (IPCC, 2001). The response of precipitation to climate forcings is, however, uncertain due to discrepancies in the magnitude and sign of climatic trends in satellite-based rainfall estimates. These discrepancies stem from systematic errors in algorithm parameters that are not explicitly measured by the observing system such as drop size distribution (DSD) in radar-based algorithms and the height of the freezing level in radiometer-based techniques. Quantifying and ultimately removing these biases is critical for studying the response of the hydrologic cycle to climate change. In addition, estimates of random errors owing to variability in algorithm assumptions on local spatial and temporal scales are critical for establishing how strongly their products should be weighted in data assimilation or model validation applications and for assigning a level confidence to climate trends diagnosed from the data.

In this paper we explore the potential for using the three-dimensional structure of radar reflectivity observations to address the problem of constraining DSD in rainfall retrievals from single-frequency radars. The method exploits the fact that distinct microphysical pathways for rainfall production often lead to differences in both the DSD of the resulting raindrops and the vertical and horizontal structure of associated radar reflectivity profiles. The primary objective of this paper is to establish the degree of consistency that can be attained in DSD parameters when rainfall is classified according to the vertical and horizontal structure of its reflectivity pattern.

## 2. RAIN-TYPE CLASSIFICATION

Conventional approaches to rain-type classification generally define two classes: (1) convective precipitation having strong updrafts, large horizontal variability, and no evidence of a bright-band (BB); and (2) horizontally homogeneous stratiform precipitation with weaker updrafts and a well-defined BB

\*Corresponding author address: Tristan S. L'Ecuyer, Department of Atmospheric Science, Colorado State University, Fort Collins, CO 80523; e-mail: tristan@atmos.colostate.edu.

at the melting level. While this approach is well-suited for estimating vertical profiles of latent heating, it is not sufficient to constrain DSDs since they can vary widely within the convective and stratiform categories themselves. The goal of this study is to use the vertical and horizontal structure of the observed radar reflectivity field to extend rain-type classification beyond convective/stratiform separation to define a larger set of rain-type classes that reduces DSD variability within each rain category. Based on preliminary analyses, the following 8 variables (illustrated in Figure 1) are adopted for defining rain-types: near-surface reflectivity, slopes between the surface and 2 km, 2-4 km, 4-6km, and 6-8km, the ratio of the maximum reflectivity in the profile to that at the surface, the highest altitude with a radar echo above 20 dBZ, and the mean horizontal gradient in surface reflectivity between the pixel and its eight nearest neighbors.

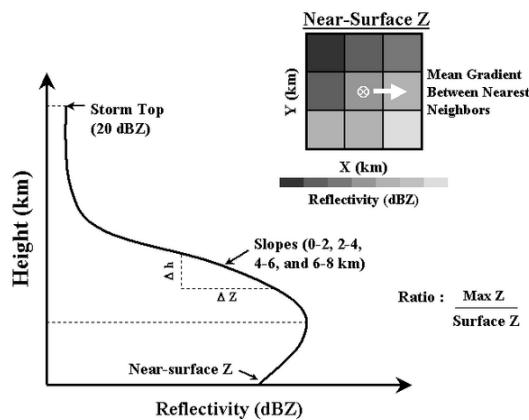


Figure 1: Variables describing the three-dimensional structure of an observed reflectivity field  $Z$  used for classifying rainfall.

The preferred resolution for these variables is that which simultaneously maximizes the amount of rainfall falling into each class and minimizes the variability of DSD within any given class. Based on ground-based polarimetric radar observations, the resolutions that define the “optimal” classification based on these criteria are presented in Table 1. Note that these dimensions result in more than 22 million possible rain-type classes but many of these classes constitute unphysical combinations of variables that are never

likely to be observed. A coarser resolution leads to fewer classes but restricts our ability to constrain DSD within each rain-type while tighter resolution makes it less likely to find similar structures thereby increasing the fraction of unclassifiable rainfall and yielding poor statistics with for determining DSD parameters appropriate to each rain-type.

Variable	Min.	Max.	$\Delta$	Bins
$Z_{sfc}$ (dBZ)	4.0	56.0	4.0	13
$S_{0-2}$	-8.0	8.0	1.0	16
$S_{2-4}$	-7.0	9.0	2.0	8
$S_{4-6}$	-15.0	5.0	2.5	8
$S_{6-8}$	-15.0	6.0	3.0	7
$Z_{max}/Z_{sfc}$	1.0	1.5	0.1	5
20 dBZ Hgt.	2.0	14.0	1.5	8
$\nabla_{XY}$	0.0	6.0	1.0	6

Table 1: The optimal classification grid. The resolution used to define rain-types is denoted  $\Delta$ . Surface reflectivity is in dBZ, the slopes, denoted  $S_{X-Y}$ , and the mean nearest-neighbor horizontal gradient, denoted  $\nabla_{XY}$ , are in dBZ km<sup>-1</sup>, the ratio of maximum to surface reflectivity is in dBZ/dBZ, and the 20 dBZ height is in km.

### 3. RESULTS FROM TRMM-LBA

To test the hypothesis that rain-type classification helps to constrain DSD, S-band polarimetric radar observations from the Tropical Rainfall Measurement Mission (TRMM)-Large-scale Biosphere Atmosphere (LBA) field experiment have been used to determine DSDs for the rain-types defined in Table 1. TRMM-LBA took place in Rondonia, Brazil during the Amazon wet season between January and February, 1999. The analyses of Rickenbach et al. (2002) (hereafter R02), Carey et al. (2001) (hereafter C01), and Petersen et al. (2002), suggest that the convection over the region falls into two distinct meteorological regimes based on the direction of the prevailing low-level winds. When easterly winds prevail, the region is characterized by significantly larger CAPE, drier lower and middle tropospheric humidity, a stronger and deeper wind shear layer, and a factor of two higher concentration of cloud condensation nuclei (CCN) than during westerly wind periods (Williams et al., 2002). C01 have also shown that raindrops in the westerly wind regime are generally smaller than those found in the easterly wind regime. Our assertion is that the properties of the DSD should be invariant within any rain-type class regardless of when it occurs. The observed differences between the easterly and westerly wind regimes should, then, be a consequence of differences in the frequency of occu-

rance of each rain-type between the regimes.

Figure 2 presents the “evolution” of rain-type classification from early atmospheric radar applications in the 1940’s to the methodology adopted here. Panel (a) represents the first meteorological radar applications in which no rain-type classification is used allowing the full range of DSD variability indicated by the broad probability density function (PDF) of  $Z_{dr}$ . Shortly thereafter, a reflectivity-based classification into convective and stratiform categories was adopted due to the fundamental differences in their microphysical, thermodynamic, and kinematic properties. Through this separation (illustrated in panel (b)), some immediate improvements in rainrate estimates were realized, primarily resulting from the reduction of biases introduced by the fact that convective raindrops are, on average, smaller than those found in stratiform rainfall. The variability of DSDs within the convective and stratiform rain-types is, however, almost as large as with no classification at all leading to potentially large uncertainties in retrieved rainfall rates.

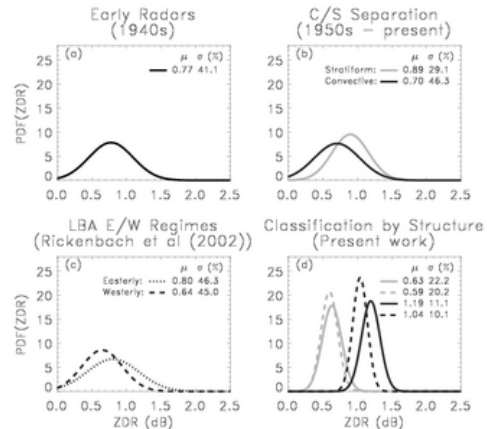


Figure 2: The evolution of rain-type classification from the 1940’s to the present. The panels present distributions of differential reflectivity,  $Z_{dr}$ , for various subsets of all TRMM-LBA radar reflectivity profiles with near-surface reflectivities of  $36 \pm 2$  dBZ.

Perhaps more importantly, this wide range of DSDs opens the door to systematic errors due to climate regime biases as can be seen in panel (c) where all convective rainfall is separated into the easterly and westerly wind regimes observed in TRMM-LBA. As reported by C01 mean drop sizes in the easterly regime are larger than those found in the westerly regime. If Z-R relationships fail to account for this, easterly rainfall will be overestimated and westerly rainfall underestimated. PDFs of  $Z_{dr}$  for two rain-type classes found in both the easterly and westerly

wind regimes are compared in panel (d). Systematic differences in mean  $Z_{dr}$ 's observed in each class differ widely from one another but these differences are captured in both synoptic regimes. Furthermore, random errors due to variability within the classes are  $\sim 75\%$  lower than those in any of the three preceding classification systems.

Overall, more than 94 % of all rain-type classes that are found in both the easterly and westerly regimes exhibit reduced variability in  $Z_{dr}$  and systematic differences in mean  $Z_{dr}$  between the easterly and westerly wind regimes are reduced more than 87 % of the time. The observed differences in synoptic conditions between the easterly and westerly wind periods in TRMM-LBA and the resulting changes in mean DSDs should, therefore, manifest themselves in the mean vertical and horizontal structure of the observed reflectivity profiles in each regime. Figure 3 compares mean easterly and westerly reflectivity profiles for all pixels with near-surface reflectivity between 34 and 38 dBZ to those corresponding to the two classes highlighted in panel (d) of Figure 2.

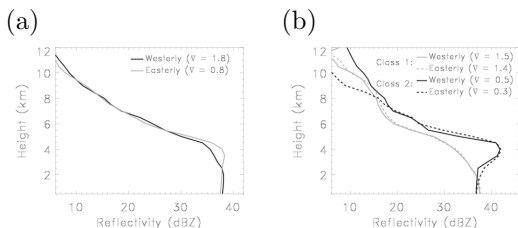


Figure 3: Mean reflectivity profiles for (a) all classes with near-surface reflectivity of  $36 (\pm 2)$  dBZ in the easterly (light) and westerly (dark) regimes of LBA, and (b) the two classes highlighted in Figure 2d, are displayed on the right. In each case, mean horizontal gradients between nearest-neighbors are provided in parentheses in the legend.

Rainfall in the easterly regime exhibits a more pronounced peak in reflectivity at 4 km, a higher melting layer, and less horizontal variability than that in the westerly regime. This is consistent with R02, C01, and Cifelli et al. (2002) who find that the easterly wind regime is characterized by a drier lower troposphere, more numerous CCN, and more abundant lightning indicative of more vigorous mixed-phase microphysics and evaporation near the surface. The reduction in the  $Z_{dr}$  bias in the two rain-types in Figure 3b can be traced to the connection between the microphysical processes governing the formation of precipitation in each case and the reflectivity profiles they produce. Class 2 exhibits a higher and more pronounced melting level, a thicker liquid water col-

umn, larger reflectivities aloft, less horizontal variability at the 1 km nearest-neighbor level, and an increase in reflectivity with height between the surface and 3 km. These characteristics suggest more vigorous mixed-phase microphysics and more evaporation at lower levels both of which result in large mean drop size and, hence, larger  $Z_{dr}$ , than Class 1. These results support the contention that differences in the mechanisms rainfall formation simultaneously manifest themselves in DSD and in the three-dimensional structure of observed reflectivity profiles providing a means for reducing differences in DSD between the easterly and westerly regimes.

#### 4. GLOBAL RAIN-TYPES

To assess the degree to which the rain-types observed in TRMM-LBA are representative of rainfall elsewhere in the tropics, TRMM PR data from the months of December 1999, January 2000, and February 2000 have been classified according to Table 1 to determine the fraction of rainfall that actually falls into classes observed in the TRMM-LBA field campaign. Figure 4 presents the fraction of rainfall that can be attributed to rain-type classes defined in TRMM-LBA for all  $5 \times 5$  degree grid box in the tropics. On average 22 % of the rainfall observed by TRMM falls into reflectivity-based rain-type categories observed in LBA. Some regions are, however, much better represented by LBA than others. Conventional wisdom would suggest that one should look to a land-based site to study continental precipitation and an ocean-based site to examine oceanic precipitation. Figure 4, on the other hand, suggests that the rainfall observed in LBA is more representative of that occurring the west pacific where almost 40 % of the local rainfall falls into classes observed in LBA than that occurring over South Africa.

To accurately assign a DSD and an associated uncertainty to a rain-type category it must, of course, be observed often enough that sufficient statistics can be accumulated to define its properties. The lowest panel of Figure 4 restricts the comparison to classes that are observed a minimum of 20 times in LBA. These rain-types characterize 3.6 % of all rainfall observed by TRMM. Noting that the LBA S-POL radar data cover only 50 days over a region that represents less than one ten-thousandth (0.0098%) of the TRMM sampling area ( $\sim 3.1 \times 10^4$  km<sup>2</sup> out of  $\sim 3.2 \times 10^8$  km<sup>2</sup>), these results are promising. Furthermore, the fact that six times as much rainfall falls into classes with fewer than 20 samples suggests that a longer field campaign in the same region could provide sufficient statistics to define the properties of a much greater fraction of tropical rainfall.

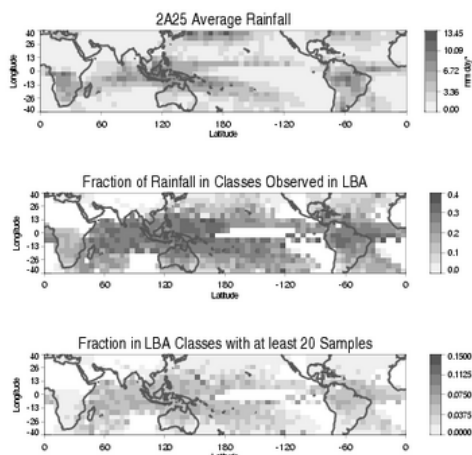


Figure 4: Mean rainfall from the PR-based 2A25 product for the months of December 1999 through February 2000 (upper panel), the fraction of this rainfall that falls into classes observed in the TRMM-LBA experiment (middle panel), and the fraction that falls into LBA-defined classes with at least 20 samples (lower panel).

## 5. DISCUSSION

The preceding analyses, while preliminary in nature, suggest that classifying rainfall by the three-dimensional structure of its reflectivity field offers the potential to reduce both random and systematic errors in DSDs assumed in rainfall retrievals. Rain-type classification also provides a means for exporting DSD deduced from polarimetric radars to those without polarization capability, such as the TRMM PR, by assigning each pixel the properties of the appropriate rain-type. In this way, biases in rainfall products arising from climate regime dependences can be partially mitigated. The fact that differences between easterly and westerly regime rainfall remain even after classification, however, implies that other factors influence DSD beyond those considered here. Further study will be required to assess the role played by aerosol type and concentration, wind shear, buoyancy, etc. in determining DSD, but, at a minimum, the technique presented here provides a template for future rain-type classification schemes.

In light of these results a new philosophy for algorithm validation emerges. Provided all algorithm assumptions are treated as soft constraints, they can be weighted according to how well they can be prescribed by auxiliary external validation. In this framework, the retrieval process can be thought of as an error-propagator which uses estimates of the uncertainties in both the measurements and assumed

parameters in conjunction with a physical model to infer a set of desired retrieval products with associated uncertainties. This approach places equal importance on assessing uncertainties in assumed parameters as it does making the observations themselves. Thus it is equally valuable to assess the mean and standard deviation of DSD assigned to a rain-type class as it is to verify the retrieved rainfall rate. If such an approach is to be adopted (eg. for future precipitation missions such as the Global Precipitation Measurement (GPM)), it will be necessary for the validation program to focus on improving the confidence in the DSDs assigned to each rain-type and representing a larger fraction of global rainfall. Through maps such as those produced in the Section 4, the method itself provides a means for assessing where validation sites need to be placed. Sites located in regions where a significant fraction of precipitation falls in rain-types not characterized by existing validation data may offer the greatest potential for filling in the properties of missing rain-types.

## 6. REFERENCES

- Carey, L. D., R. Cifelli, W. A. Petersen, S. A. Rutledge, and M. A. F. Silva Dias, 2001: Characteristics of Amazonian Rain Measured During TRMM-LBA, *Preprints from the 30th International Conf. on Radar Meteorology, Munich, Germany*, Amer. Meteor. Soc., 682-684.
- Cifelli, R., W. A. Petersen, L. D. Carey, and S. A. Rutledge, 2002: Radar observations of the kinematic, microphysical, and precipitation characteristics of two MCS's in TRMM-LBA, *J. Geophys. Res.*, **107**, doi:10.1029/2000JD000264.
- IPCC Working Group II, 2001: *Climate Change 2001: Impacts and Vulnerability*, Intergovernmental Panel on Climate Change (IPCC), World Meteorological Office, United Nations Environmental Programme.
- Petersen, W. A., S. W. Nesbitt, R. J. Blakeslee, R. Cifelli, P. Hein, and S. A. Rutledge, 2002: TRMM Observations of Intraseasonal Variability in Convective Regimes over the Amazon, *Climate Dynamics*, **15**, 1278-1294.
- Rickenbach, T. M., R. N. Ferreira, J. Halverson, and M. A. F. Silva Dias, 2002: Mesoscale properties of convection in Western Amazonia in the context of large-scale wind regimes, *J. Geophys. Res.*, **107**, doi:10.1029/2000JD000263.
- Williams, E. and co-authors, 2002: The Green Ocean over the Amazon, *J. Geophys. Res.*, **107**, doi:10.1029/2001JD000380.